



Selenium-Curcumin-PEG Nanoparticles Radiosensitization for Intensity-Modulated Radiation Therapy of Lung Tumor Cells: *In Vitro* Synergistic Combination Therapy

Farid Mortazavi (MSc Student)^{1,2}, Paria Tamaddon (MSc)², Ali Ketabi (PhD)^{1,3}, Hanieh Haghighi (MSc)¹, Kiana Khajeheian (MSc)², Masoud Haghani (PhD)^{1,4}, Tahereh Mahmoudi (PhD)^{1,2}, Sadegh Masjoodi (PhD)⁵, Masoud Negahdary (PhD)^{6,7}, Naghmeh Sattarahmady (PhD)^{1,2}

ABSTRACT

Background: Lung cancer is a leading cause of cancer-related mortality worldwide, underscoring the need for the development of more effective treatment strategies. Radiotherapy (RT), particularly intensity-modulated radiation therapy (IMRT), has enhanced tumor targeting while minimizing damage to healthy tissues. Nevertheless, radioresistance and challenges posed by the tumor microenvironment limit its efficacy.

Objective: Selenium-curcumin-polyethylene glycol 600 nanoparticles (Se-Cur-PEG NPs) analyzed as radiosensitizers in IMRT for lung cancer treatment.

Material and Methods: In this experimental study, Se-Cur-PEG NPs were synthesized and characterized for their potential as radiosensitizers.

Results: The *in vitro* toxicity of Se-Cur-PEG NPs against A549 lung cancer cells was evaluated using MTT assays, demonstrating a dose-dependent reduction in cell viability. The combination of Se-Cur-PEG NPs (50 $\mu\text{g mL}^{-1}$) with IMRT (4 Gy) resulted in a significant enhancement in cell death compared to either treatment alone, indicating a strong synergistic effect (CI=1.21) and a notable sensitizer enhancement ratio (SER=2.5). Intracellular ROS generation analysis confirmed that Se-Cur-PEG NPs amplified IMRT-induced oxidative stress, contributing to increased cancer cell toxicity.

Conclusion: These findings suggest that Se-Cur-PEG NPs hold promise as effective radiosensitizers, potentially improving lung cancer RT outcomes.

Keywords

Intensity-Modulated; Lung Neoplasms; Selenium nanoparticles; Oxidative Stress; Radiation-Sensitizing Agents

Introduction

Cancer continues to pose a formidable challenge to global health, with lung cancer-clinically referred to as bronchogenic carcinoma- emerging as one of the most prevalent and lethal forms. This malignancy originates from the lung parenchyma or bronchial tubes and has witnessed a dramatic increase in incidence over the past

¹Nanomedicine and Nanobiology Research Center, Shiraz University of Medical Sciences, Shiraz, Iran

²Department of Medical Physics and Engineering, School of Medicine, Shiraz University of Medical Sciences, Shiraz, Iran

³Physics Unit, Department of Radio-oncology, School of Medicine, Shiraz University of Medical Sciences, Shiraz, Iran

⁴Department of Radiology, School of Paramedical Science, Shiraz University of Medical Sciences, Shiraz, Iran

⁵Neuroscience Research Centre, Shiraz University of Medical Sciences, Shiraz, Iran

⁶Department of Biomedical Engineering, Texas A&M University, 600 Discovery Drive, College Station, TX, 77840-3006, USA

⁷Center for Remote Health Technologies & Systems, Texas A&M Engineering Experiment Station, 600 Discovery Drive, College Station, TX, 77840-3006, USA

*Corresponding author: Naghmeh Sattarahmady Nanomedicine and Nanobiology Research Center, Shiraz University of Medical Sciences, Shiraz, Iran
E-mail: nsattar@sums.ac.ir

Received: 10 February 2025
Accepted: 24 February 2024

century, primarily attributed to the widespread adoption of smoking among both genders [1]. Despite advances in therapeutic modalities, including immunotherapy, chemotherapy, ablative techniques, radiotherapy (RT), and targeted therapies, these interventions often result in significant side effects and limited efficacy, underscoring the need for innovative treatment approaches [2-5].

Among existing modalities, RT has established itself as a cornerstone in the treatment of various cancers, including lung cancer, due to its ability to penetrate tissues deeply and deliver targeted cytotoxic effects to tumors [6]. However, conventional RT is hindered by significant limitations, such as dose heterogeneity, toxicity to adjacent healthy tissues, and complications such as radiation pneumonitis (RP) [7]. To overcome these challenges, intensity-modulated radiation therapy (IMRT) has emerged as an advanced RT technique, capable of delivering highly precise radiation doses by conforming to the tumor's shape while sparing healthy tissues. IMRT has demonstrated superior outcomes, including reduced rates of RP, enhanced locoregional tumor control, and improved patient quality of life compared to traditional RT [8]. In particular, IMRT has shown promising results for patients with inoperable non-small cell lung cancer (NSCLC), significantly improving local control and minimizing radiation-induced complications [9].

Despite these advancements, the tumor microenvironment (TME) presents substantial barriers to treatment success. Characteristics such as hypoxia, elevated interstitial pressure, and compromised blood flow reduce radiosensitivity and hinder the delivery of therapeutic agents, thereby limiting the efficacy of RT [10]. Furthermore, the presence of radioresistance and prolonged exposure of healthy tissues to radiation highlight the necessity for adjuvant approaches to enhance treatment outcomes [11].

Nanotechnology has revolutionized the field

of cancer therapy, offering innovative platforms that enhance the efficacy and specificity of treatments [4,5, 12-14]. Among these advancements, selenium nanoparticles (NPs) have garnered significant attention due to their selective toxicity, inducing apoptosis in cancer cells via reactive oxygen species (ROS) generation while sparing healthy tissues [15]. Functionalized selenium NPs, such as selenium-polyethylene glycol-curcumin, combine the unique properties of selenium, polyethylene glycol, and curcumin, creating a potent therapeutic agent for improving RT outcomes [16].

Selenium, a trace element with powerful antioxidant and anticancer properties, enhances oxidative stress in tumor cells, sensitizing them to radiation while modulating immune responses and inhibiting angiogenesis [7,17]. Polyethylene glycol improves the biocompatibility and stability of nanoparticles, prolonging circulation time and enabling efficient tumor targeting by minimizing immune clearance [10]. Curcumin, a bioactive polyphenol, provides a broad spectrum of anticancer effects, including the inhibition of cell proliferation, induction of apoptosis, and suppression of metastasis. Notably, curcumin synergistically amplifies ROS generation during RT, intensifying oxidative stress in cancer cells while offering cytoprotective effects to healthy tissues [18].

The integration of Se-Cur-PEG NPs into IMRT protocols addresses several limitations of conventional RT by improving tumor radiosensitivity, overcoming barriers within the TME, and minimizing collateral damage to healthy tissues. These advancements highlight the potential of combining precision RT techniques with innovative nanomaterials to revolutionize the treatment of lung cancer [19-21].

In the present study, Se-Cur-PEG NPs were synthesized and comprehensively physicochemically characterized. Their therapeutic potential in eradicating lung cancer cells

was systematically evaluated under IMRT. Emphasis was placed on their capacity to enhance ROS generation in response to IMRT.

Material and Methods

Materials

In this experimental research, the following materials were procured from Scharlau (Spain): polyethylene glycol 600 (PEG 600), dimethyl sulfoxide (DMSO), ascorbic acid, and sodium selenite. 3-(4,5-Dimethylthiazol-2-yl)-2,5-diphenyltetrazolium bromide (MTT) and 2'-7'-dichlorodihydrofluorescein diacetate (DCFH-DA) were acquired from Sigma-Aldrich (USA). Curcumin was obtained from Merck KGaA (Germany). Deionized (DI) water was utilized in all experimental procedures.

Synthesis of Se-Cur-PEG NPs

A sodium selenite (Na_2SeO_3) solution with a concentration of 1 mg mL^{-1} was prepared by dissolving the compound in distilled water. Subsequently, a solution of PEG 600 that contained curcumin (80 mg mL^{-1}) was incorporated into the aforementioned mixture. Additionally, an ascorbic acid solution (12 mg mL^{-1}) was introduced dropwise into the mixture, which was continuously stirred for a duration of 24 h. Next, the mixture underwent centrifugation at 8000 rpm for 30 min, yielding a brick-red colored supernatant. The resultant solution was subjected to multiple washes with a cold ethanol-water mixture to eliminate any unbound curcumin. Following this purification step, the solution was rinsed several times with distilled water to remove unreacted components, including ascorbic acid and Na_2SeO_3 . Eventually, the nanoparticles were lyophilized and stored at 4°C for future applications.

Characterization of Se-Cur-PEG NPs

The UV-vis absorption spectrum of Se-Cur-PEG NPs was acquired employing a Rayleigh

double beam spectrophotometer (China). The morphology of Se-Cur-PEG NPs was evaluated via field emission scanning electron microscopy (FESEM) utilizing a Zeiss Sigma-IGMA/VP instrument (Germany). Following this, zeta potential of the Se-Cur-PEG suspensions was quantified using the SZ-100 instrument manufactured by HORIBA (Japan).

Cell line preparation

The lung cancer cells (A549) were purchased from the Pasteur Institute (Iran). The cells were cultured in standard Dulbecco's Modified Eagle Medium (DMEM) supplied by Gibco (USA), which was supplemented with 10% fetal bovine serum (FBS) and 1% antibiotic solution (Pen-Strep) containing penicillin and streptomycin, also sourced from Gibco (USA). The cultures were maintained at a temperature of 37°C in a humidified atmosphere containing 5% CO_2 .

A549 cytotoxicity in the presence of Se-Cur-PEG NPs

To assess the cytotoxicity of the A549 cell line, 1.0×10^4 cells were seeded into microplate wells containing $100 \mu\text{L}$ of supplemented DMEM media and incubated for a period of 24 h to allow adherence to the wells. This was followed by an overnight exposure to Se-Cur-PEG NPs at concentrations of 0, 5, 10, 25, 50, and $100 \mu\text{g mL}^{-1}$, with untreated cells acting as the control group. Cell toxicity was evaluated utilizing the MTT proliferation assay; following treatment, the media were substituted with MTT solution (0.5 mg mL^{-1} , $100 \mu\text{L}$ in phosphate-buffered saline), and cells were incubated in the darkness for 4 h. Subsequently, the MTT solution was removed, and $100 \mu\text{L}$ of DMSO was added. After a 30 min incubation period, the microplates were subjected to centrifugation at 1800 rpm for 10 min. The optical density (OD) of each well was measured at a wavelength of 570 nm using a Stat Fax microplate reader (USA), with untreated cells serving as the control group.

for all assessments. To determine cell viability, the uptake ratio in each well was calculated relative to the control, and each concentration was evaluated in triplicate to ensure accuracy. Furthermore, the half-maximal inhibitory concentration (IC50) for Se-Cur-PEG NPs was derived from the analysis of sigmoid dose-response curves.

Radiotherapy exposure of A549 in the presence of Se-Cur-PEG NPs

The RT protocol involved the administration of radiation dose of 4 Gy at a rate of 1000 units per min, utilizing IMRT with an Accuray Radixact device (USA). This methodology required the positioning of a 3 cm slab above the plate and a 2 cm slab below it, with the aim of focusing on the central region of the cell culture plate.

The IC50 value derived from the sigmoid dose-response curves of Se-Cur-PEG NPs was used to treat A549 cells. These cells were exposed to the IC50 concentration ($50 \mu\text{g mL}^{-1}$) of Se-Cur-PEG NPs and after a 24 h incubation combined with IMRT at a dose of 4 Gy, delivered at a rate of 1000 units per min. This treatment was administered as a stand-alone intervention control group. Cell toxicity was evaluated utilizing the MTT proliferation assay.

The sensitizer enhancement ratio (SER) was also determined by comparing cell viability following IMRT radiation at a dose of 4 Gy, under conditions both standalone and in conjunction with Se-Cur-PEG NPs.

Analysis of ROS generation

In vitro IMRT treatment of A549 cells was conducted 24 h post-seeding to evaluate intracellular ROS generation using Se-Cur-PEG NPs. These cells were exposed to the IC50 concentration ($50 \mu\text{g mL}^{-1}$) of Se-Cur-PEG NPs, standalone and in conjunction with IMRT treatment. After a 1 h incubation, 100 μL of a freshly prepared solution of DCFH-DA at a concentration of $50 \mu\text{mol L}^{-1}$ was

added to each sample. The cells were then incubated for an additional 30 min, followed by three washes with PBS (20 mmol L^{-1} , pH 7.4). Subsequently, 100 μL of lysis buffer, comprising NaCl, Triton X-100, and Tris-HCl (pH 8.0), was added to each well.

Fluorescence intensity (F.I.) at 520 nm was measured using a Biotek microplate reader (USA) with an excitation wavelength of 485 nm. All measurements were conducted on 96-well black plates, with PBS serving as the control.

Evaluation of domination of synergism effects

The impact of synergistic interactions on the treatment of A549 cells with IMRT and Se-Cur-PEG NPs was evaluated by calculating combination indices (CIs). When two factors, A and B, influence cell toxicity either separately or simultaneously, the following formula is used to determine the CIs [22]:

$$CI = V_A \times V_B / V_{AB} \quad (\text{Eq. 1})$$

In this equation, the variables V_A and V_B denote the cell viability resulting from the individual treatments A and B, respectively. In contrast, V_{AB} indicates the cell viability observed when both treatments are administered simultaneously. CI values that exceed, equal, or fall below 1 reflect the nature of interactions between the treatments. Specifically, values greater than 1 suggest a synergistic effect, values equal to 1 denote an additive effect, and values less than 1 indicate an antagonistic effect [23].

Statistical analysis

The statistical analyses were conducted using GraphPad Prism 9 software. The findings were reported as means accompanied by standard deviations, derived from a minimum of three independent measurements for each experiment. In order to assess the significance of the results, both the two-tailed Student's t-test and the non-parametric Kruskal-Wallis test were employed. In this context, a *P*-value

of less than 0.05 was considered to be statistically significant.

Results

Characterization of Se-Cur-PEG NPs

The UV-vis absorption spectrum of the synthesized Se-Cur-PEG NPs, shown in Figure 1, reveals distinct peaks and features that highlight the optical properties of these nanostructures. A notable peak in the range of 200-240 nm suggests the presence of the PEG component [24]. Meanwhile, the broader peaks at longer wavelengths are attributed to the interactions between selenium and curcumin within the Se-Cur-PEG structure. The zeta potential of Se-Cur-PEG NPs was assessed, yielding a result of -38.4 mV with an electrophoretic mobility of $-0.000297 \text{ cm}^2 \text{ V}^{-1} \text{ s}^{-1}$. This zeta potential value indicates a significant level of stability for the Se-Cur-PEG NPs, thereby preventing the occurrence of aggregation.

Figure 2 presents a FESEM image of Se-Cur-PEG NPs. The dimensions of the nanoparticles were assessed for 50 particles ($n=50$), with the scale in the image indicating a pixel-to-micron conversion factor of approximately 10.2 pixels per micron. The

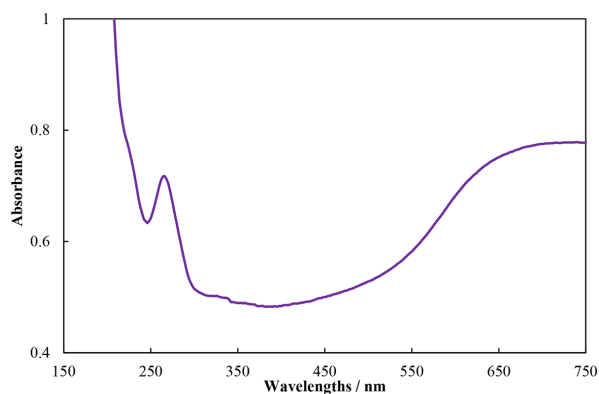


Figure 1: Characteristic UV-vis absorption spectrum of Selenium-curcumin-polyethylene glycol 600 nanoparticles (Se-Cur-PEG NPs).

Se-Cur-PEG NPs exhibited an average diameter of $70 \pm 12 \text{ nm}$. This size is particularly advantageous for uptake by the A549 cell line, which is a human lung carcinoma epithelial cell line frequently employed in oncological research. Nanoparticles of this size are generally effective in cellular internalization through endocytosis, thereby improving the efficacy of drug delivery and facilitating extended circulation [25,26].

A549 cell viability

In this study, the cytotoxic effects of Se-Cur-PEG NPs and IMRT were aimed at being evaluated through MTT assays, both individually and in combination, *in vitro*. As illustrated in Figure 3 (A), Se-Cur-PEG NPs significantly diminished cellular viability in a dose-dependent fashion when compared to the untreated control group after a 24 h exposure period. The findings suggest that Se-Cur-PEG NPs exhibit low cytotoxicity at concentrations up to $10 \mu\text{g mL}^{-1}$; however, at

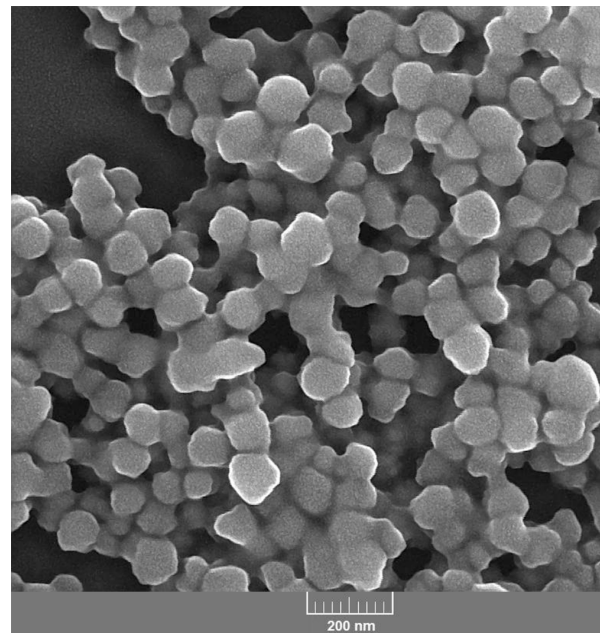


Figure 2: A field emission scanning electron microscopy (FESEM) image of Selenium-curcumin-polyethylene glycol 600 nanoparticles (Se-Cur-PEG NPs).

25 $\mu\text{g mL}^{-1}$, cell viability fell below 60.0%, reaching approximately 39.0% at the highest concentration tested. A concentration of 50 $\mu\text{g mL}^{-1}$ was determined to be the IC₅₀ value for Se-Cur-PEG NPs in A549 cells, resulting in a viability rate of 46.7%. Further investigation into the toxicological characteristics of Se-Cur-PEG NPs indicated that at 5 $\mu\text{g mL}^{-1}$, cell viability remained around 80% after 24 h of treatment, implying a relatively low toxicity threshold.

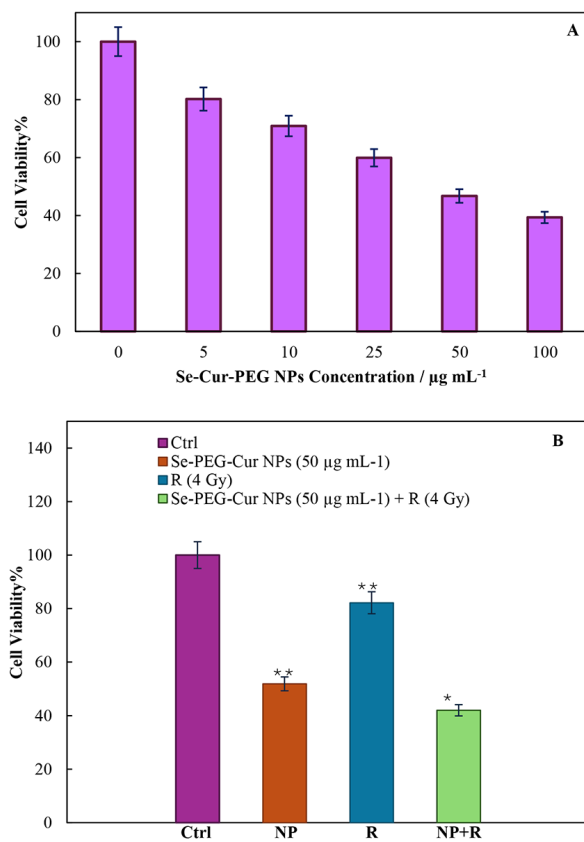


Figure 3: Assessment of A549 lung cancer cell viability following treatment with A) varying concentrations of Selenium-curcumin-polyethylene glycol 600 nanoparticles (Se-Cur-PEG NPs) over a 24 h period. B) Treatment with Se-Cur-PEG NPs at the inhibitory concentration (IC₅₀) of 50 $\mu\text{g mL}^{-1}$ for 24 h, followed by intensity-modulated radiation therapy (IMRT) irradiation at a dose of 4 Gy. **denotes statistically significant differences (P -value<0.01).

As illustrated in Figure 3 (B), the viability of A549 cells was evaluated following exposure to IMRT (R₄ Gy) and Se-Cur-PEG NPs (NP, 50 $\mu\text{g mL}^{-1}$) after 48 h, both as individual treatments and in combination (NP+R₄ Gy). The MTT assay results demonstrated that A549 cells subjected to IMRT alone exhibited a survival rate of approximately 90%. Conversely, the combination of IMRT and Se-Cur-PEG NPs (50 $\mu\text{g mL}^{-1}$) resulted in a significant decline in cell viability, reaching 35.0%.

Assessment of intracellular ROS production in A549 cells

As illustrated in Figure 4, Se-Cur-PEG NPs demonstrated a significant ability to enhance intracellular ROS production, as reflected by the F.I. of DCF, a widely recognized indicator of intracellular ROS levels. The data suggest that Se-Cur-PEG NPs substantially increased ROS generation within the cells.

Discussion

Numerous sensitizers demonstrate significant radiosensitizing capabilities, thereby

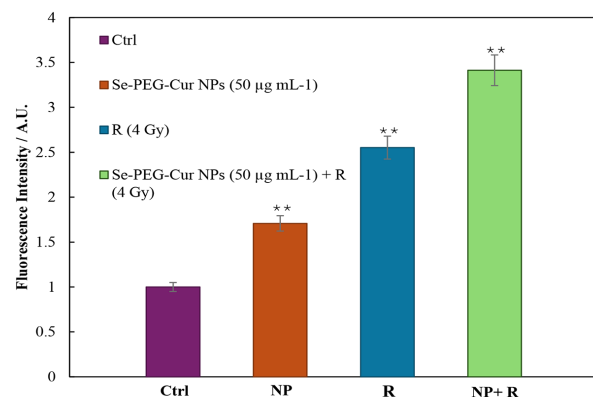


Figure 4: Measurement of fluorescence intensity (F.I.) of 2',7'-dichlorodihydrofluorescein (DCF) subsequent to incubation with Selenium-curcumin-polyethylene glycol 600 nanoparticles (Se-Cur-PEG NPs) (IC₅₀, 50 $\mu\text{g mL}^{-1}$) and IMRT irradiation (4 Gy) within A549 lung cancer cells. **indicates highly significant differences (P -value<0.001).

enhancing the therapeutic effectiveness of RT [27,28]. The unique physicochemical properties of Se-Cur-PEG NPs- namely their biocompatibility, stability, and ability to modulate oxidative stress within the cellular environment- indicate a substantial potential for these nanoparticles to serve as effective radiosensitizers [16,21]. In this investigation, Se-Cur-PEG NPs were synthesized, thoroughly characterized, and assessed for their radiosensitizing effects both standalone and in conjunction with ionizing radiation. The synergistic interactions of these nanoparticles with IMRT were meticulously evaluated, particularly using the A549 cell line. Moreover, the individual and combinatorial applications of Se-Cur-PEG NPs alongside IMRT were investigated to elucidate their mechanistic roles in enhancing the generation of ROS and inducing cytotoxicity. This comprehensive approach highlights the potential of Se-Cur-PEG NPs to optimize radiotherapeutic outcomes in a targeted and efficient manner.

The viability results indicate a substantial synergistic interaction between nanoparticle-based therapy and radiation, suggesting that Se-Cur-PEG NPs act as effective radiosensitizers, thereby enhancing the therapeutic efficacy of IMRT. It is noteworthy that the combination of these treatments resulted in an additional 11.7% reduction in cellular viability compared to IMRT alone, which underscores the potential of Se-Cur-PEG NPs to potentiate radiation-induced cellular toxicity. Also, SER value was 2.5 that indicates an effective role of Se-Cur-PEG NPs as radiosensitizer. This enhancement is likely attributable to the ability of selenium-based nanoparticles to amplify oxidative stress and disrupt intracellular redox homeostasis, thereby augmenting radiation-induced DNA damage and impairing cellular repair mechanisms [29,30]. Furthermore, calculation of CI values in the context of Se-Cur-PEG NPs at a radiation dose of R_4 Gy (CI=1.21) exceeded 1, indicating that a synergistic effect has been established.

Notably, cells subjected to IMRT exhibited an elevated ROS production capacity, and the combination of IMRT with Se-Cur-PEG NPs yielded the highest intracellular ROS levels. These findings align with prior *in vitro* investigations demonstrating that increased ROS generation correlates with reduced cancer cell viability following nanoparticle-based radiosensitization [31].

Conclusion

This study demonstrated that Se-Cur-PEG NPs significantly enhance the efficacy of IMRT in lung cancer treatment. The nanoparticles exhibited strong cytotoxic effects against A549 lung cancer cells in a dose-dependent fashion, with an IC50 of 50 $\mu\text{g mL}^{-1}$. The combination of IMRT and Se-Cur-PEG NPs resulted in a synergistic increase in cancer cell death, as evidenced by CI analysis. Furthermore, ROS generation assays demonstrated that these nanoparticles amplified oxidative stress induced by IMRT, a pivotal mechanism in radiosensitization. These findings underscore the potential of Se-Cur-PEG NPs as a promising adjuvant in RT, promising enhanced therapeutic outcomes for lung cancer patients.

Acknowledgment

We express our gratitude to the Research Council of Shiraz University of Medical Sciences (31317) for their financial assistance in supporting this research.

Authors' Contribution

N. Sattarahmady and A. Ketabi contributed to the study conception and design. N. Sattarahmady conceived the original idea and supervised the project. A. Ketabi, M. Negahdary, P. Tamaddon, and H. Haghighi played a pivotal role in designing the procedure and fabrication of the nanoparticles. Material preparation, data collection, and analysis were performed by F. Mortazavi, P. Tamaddon, K. Khajeheian, M. Haghani, T. Mahmoudi, and

S. Masjoodi, F. Mortazavi and P. Tamaddon equally contributed to this work. All authors actively contributed in writing and reviewing the manuscript, ensuring a comprehensive and well-rounded study. All authors read, modified, and approved the final version of the manuscript.

Ethical Approval

The national ethics committee confirmed the study with the ethical code of IR.SUMS.REC.1403.270. We did not perform any intervention in therapeutic procedures. Therefore, gathering the consent forms was waived due to the nature of this study.

Funding

This work was supported by Shiraz University of Medical Sciences (Shiraz, Iran) with the grant number of “31317”.

Conflict of Interest

N. Sattarahmady, as the Editorial Board Member, was not involved in the peer-review and decision-making processes for this manuscript.

References

1. Nasim F, Sabath BF, Eapen GA. Lung Cancer. *Med Clin North Am*. 2019;**103**(3):463-73. doi: 10.1016/j.mcna.2018.12.006. PubMed PMID: 30955514.
2. Król K, Mazur A, Stachyra-Strawa P, Grzybowska-Szatkowska L. Non-Small Cell Lung Cancer Treatment with Molecularly Targeted Therapy and Concurrent Radiotherapy-A Review. *Int J Mol Sci*. 2023;**24**(6):5858. doi: 10.3390/ijms24065858. PubMed PMID: 36982933. PubMed PMCID: PMC10052930.
3. Jumeau R, Vilotte F, Durham AD, Ozsahin EM. Current landscape of palliative radiotherapy for non-small-cell lung cancer. *Transl Lung Cancer Res*. 2019;**8**(Suppl 2):S192-201. doi: 10.21037/tlcr.2019.08.10. PubMed PMID: 31673524. PubMed PMCID: PMC6795576.
4. Perota G, Faghani-Eskandarkolaei P, Zahraie N, Zare MH, Sattarahmady N. A Study of Sonodynamic Therapy of Melanoma C540 Cells in Vitro by Titania/Gold Nanoparticles. *J Biomed Phys Eng*. 2024;**14**(1):43-54. doi: 10.31661/jbpe.v0i0.2310-1674. PubMed PMID: 38357599. PubMed PMCID: PMC10862114.
5. Kayani Z, Heli H, Dehdari Vais R, Haghighi H, Ajdari M, Sattarahmady N. Synchronized Chemotherapy/Photothermal Therapy/Sonodynamic Therapy of Human Triple-Negative and Estrogen Receptor-Positive Breast Cancer Cells Using a Doxorubicin-Gold Nanoclusters-Albumin Nanobioconjugate. *Ultrasound Med Biol*. 2024;**50**(6):869-81. doi: 10.1016/j.ultrasmedbio.2024.02.012. PubMed PMID: 38538442.
6. Kirsch DG, Diehn M, Kesarwala AH, Maity A, Morgan MA, Schwarz JK, et al. The Future of Radiobiology. *J Natl Cancer Inst*. 2018;**110**(4):329-40. doi: 10.1093/jnci/djx231. PubMed PMID: 29126306. PubMed PMCID: PMC5928778.
7. Shirai K, Aoki S, Endo M, Takahashi Y, Fukuda Y, Akahane K, et al. Recent developments in the field of radiotherapy for the management of lung cancer. *Jpn J Radiol*. 2025;**43**(2):186-99. doi: 10.1007/s11604-024-01663-8. PubMed PMID: 39316285. PubMed PMCID: PMC11790782.
8. Taylor A, Powell ME. Intensity-modulated radiotherapy--what is it? *Cancer Imaging*. 2004;**4**(2):68-73. doi: 10.1102/1470-7330.2004.0003. PubMed PMID: 18250011. PubMed PMCID: PMC1434586.
9. Sura S, Gupta V, Yorke E, Jackson A, Amols H, Rosenzweig KE. Intensity-modulated radiation therapy (IMRT) for inoperable non-small cell lung cancer: the Memorial Sloan-Kettering Cancer Center (MSKCC) experience. *Radiother Oncol*. 2008;**87**(1):17-23. doi: 10.1016/j.radonc.2008.02.005. PubMed PMID: 18343515. PubMed PMCID: PMC2722446.
10. Bensenane R, Helfre S, Cao K, Carton M, Champion L, Girard N, et al. Optimizing lung cancer radiation therapy: A systematic review of multifactorial risk assessment for radiation-induced lung toxicity. *Cancer Treat Rev*. 2024;**124**:102684. doi: 10.1016/j.ctrv.2024.102684. PubMed PMID: 38278078.
11. Chen G, Wu K, Li H, Xia D, He T. Role of hypoxia in the tumor microenvironment and targeted therapy. *Front Oncol*. 2022;**12**:961637. doi: 10.3389/fonc.2022.961637. PubMed PMID: 36212414. PubMed PMCID: PMC9545774.
12. Heli H, Rahi A. Synthesis and Applications of Nanoflowers. *Recent Pat Nanotechnol*. 2016;**10**(2):86-115. doi: 10.2174/1872210510999160517102102. PubMed PMID: 27502388.

13. Ajdari M, Ranjbar A, Karimian K, Karimi M, Heli H, Sattarahmady N. Characterization and Evaluation of Nano-niosomes Encapsulating Docetaxel against Human Breast, Pancreatic, and Pulmonary Adenocarcinoma Cancer Cell Lines. *J Biomed Phys Eng*. 2024;**14**(2):159-68. doi: 10.31661/jbpe.v0i0.2401-1708. PubMed PMID: 38628892. PubMed PMCID: PMC11016824.
14. Karimi M, Karimian K, Heli H. A nanoemulsion-based delivery system for imatinib and in vitro anticancer efficacy. *Braz J Pharm Sci*. 2020;**56**:e18973. doi: 10.1590/s2175-97902020000118973.
15. Sampath S, Sunderam V, Manjusha M, Dlamini Z, Lawrance AV. Selenium Nanoparticles: A Comprehensive Examination of Synthesis Techniques and Their Diverse Applications in Medical Research and Toxicology Studies. *Molecules*. 2024;**29**(4):801. doi: 10.3390/molecules29040801. PubMed PMID: 38398553. PubMed PMCID: PMC10893520.
16. Mohammadi S, Soratijahromi E, Dehdari Vais R, Sattarahmady N. Phototherapy and Sono-therapy of Melanoma Cancer Cells Using Nanoparticles of Selenium-Polyethylene Glycol-Curcumin as a Dual-Mode Sensitizer. *J Biomed Phys Eng*. 2020;**10**(5):597-606. doi: 10.31661/jbpe.v0i0.1912-1039. PubMed PMID:33134219. PubMed PMCID: PMC7557466.
17. Sharma A, Shambhwani D, Pandey S, Singh J, Lalhlenmawia H, Kumarasamy M, et al. Advances in Lung Cancer Treatment Using Nanomedicines. *ACS Omega*. 2022;**8**(1):10-41. doi: 10.1021/acsomega.2c04078. PubMed PMID: 36643475. PubMed PMCID: PMC9835549.
18. Slama Y, Arcambal A, Septembre-Malaterre A, Morel AL, Pesnel S, Gasque P. Evaluation of core-shell Fe₃O₄@Au nanoparticles as radioenhancer in A549 cell lung cancer model. *Heliyon*. 2024;**10**(8):e29297. doi: 10.1016/j.heliyon.2024.e29297. PubMed PMID: 38644868. PubMed PMCID: PMC11033100.
19. Wang J, Zhou T, Liu Y, Chen S, Yu Z. Application of Nanoparticles in the Treatment of Lung Cancer With Emphasis on Receptors. *Front Pharmacol*. 2022;**12**:781425. doi: 10.3389/fphar.2021.781425. PubMed PMID: 35082668. PubMed PMCID: PMC8785094.
20. Carrasco-Esteban E, Domínguez-Rullán JA, Barionuevo-Castillo P, Pelari-Mici L, Leaman O, Sastre-Gallego S, López-Campos F. Current role of nanoparticles in the treatment of lung cancer. *J Clin Transl Res*. 2021;**7**(2):140-55. PubMed PMID: 34104817. PubMed PMCID: PMC8177846.
21. Ilbeigi S, Ranjbar A, Zahraie N, Vais RD, Monjezi MR, Sattarahmady N. Sonodynamic therapy of pancreatic cancer cells based on synergistic chemotherapeutic effects of selenium-PEG-curcumin nanoparticles and gemcitabine. *Appl Phys A*. 2023;**129**(2):82. doi: 10.1007/s00339-022-06377-0.
22. Foucquier J, Guedj M. Analysis of drug combinations: current methodological landscape. *Pharmacol Res Perspect*. 2015;**3**(3):e00149. doi: 10.1002/prp2.149. PubMed PMID: 26171228. PubMed PMCID: PMC4492765.
23. Chou TC. Drug combination studies and their synergy quantification using the Chou-Talalay method. *Cancer Res*. 2010;**70**(2):440-6. doi: 10.1158/0008-5472.CAN-09-1947. PubMed PMID: 20068163.
24. Haghghi H, Zahraie N, Haghani M, Heli H, Sattarahmady N. An amplified sonodynamic therapy by a nanohybrid of titanium dioxide-gold-polyethylene glycol-curcumin: HeLa cancer cells treatment in 2D monolayer and 3D spheroid models. *Ultrason Sonochem*. 2024;**102**:106747. doi: 10.1016/j.ultsonch.2023.106747. PubMed PMID: 38154206. PubMed PMCID: PMC10765485.
25. Ireland G, Simmons R, Hickman M, Eastwood B, Ramsay M, Mandal S. Mapping the hepatitis C cascade of care in people attending drug treatment services in England: A data linkage study. *Int J Drug Policy*. 2019;**72**:55-60. doi: 10.1016/j.drugpo.2019.06.006. PubMed PMID: 31257040.
26. Nazari-Vanani R, Kayani Z, Karimian K, Ajdari MR, Heli H. Development of New Nanoniosome Carriers for Vorinostat: Evaluation of Anticancer Efficacy In Vitro. *J Pharm Sci*. 2024;**113**(8):2584-94. doi: 10.1016/j.xphs.2024.05.025. PubMed PMID: 38801974.
27. Gong L, Zhang Y, Liu C, Zhang M, Han S. Application of Radiosensitizers in Cancer Radiotherapy. *Int J Nanomedicine*. 2021;**16**:1083-102. doi: 10.2147/IJN.S290438. PubMed PMID: 33603370. PubMed PMCID: PMC7886779.
28. Boateng F, Ngwa W. Delivery of Nanoparticle-Based Radiosensitizers for Radiotherapy Applications. *Int J Mol Sci*. 2019;**21**(1):273. doi: 10.3390/ijms21010273. PubMed PMID: 31906108. PubMed PMCID: PMC6981554.
29. Ferro C, Florindo HF, Santos HA. Selenium Nanoparticles for Biomedical Applications: From Development and Characterization to Therapeutics. *Adv Healthc Mater*. 2021;**10**(16):e2100598. doi: 10.1002/adhm.202100598. PubMed PMID:

- 34121366.
30. Deng X, Ouyang P, Xu W, Yang E, Bao Z, Wu Y, et al. Research progress of nano selenium in the treatment of oxidative stress injury during hepatic ischemia-reperfusion injury. *Front Pharmacol.* 2023;**13**:1103483. doi: 10.3389/fphar.2022.1103483. PubMed PMID: 36686647. PubMed PMCID: PMC9846509.
31. Zhao G, Wu X, Chen P, Zhang L, Yang CS, Zhang J. Selenium nanoparticles are more efficient than sodium selenite in producing reactive oxygen species and hyper-accumulation of selenium nanoparticles in cancer cells generates potent therapeutic effects. *Free Radic Biol Med.* 2018;**126**:55-66. doi: 10.1016/j.freeradbiomed.2018.07.017. PubMed PMID: 30056082.